

# A Novel Crystal Growth Model with Nonlinear Interface Kinetics and Curvature Effects: Sensitivity Analysis and Optimization

Saad Akhtar, Minghan Xu, and Agus P. Sasmito\*

Cite This: <https://doi.org/10.1021/acs.cgd.0c01652>

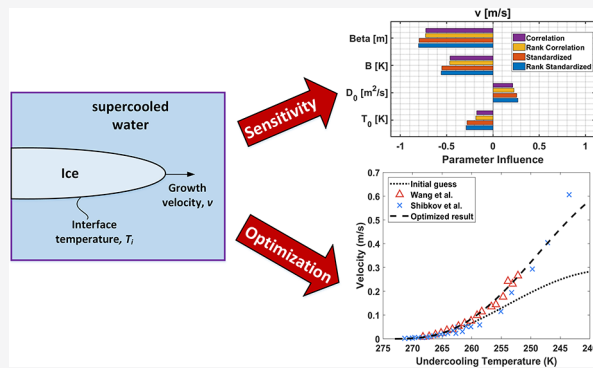
Read Online

ACCESS |

Metrics &amp; More

Article Recommendations

**ABSTRACT:** With the ever-increasing engineering and biological applications of rapid droplet solidification on superhydrophobic surfaces, developing accurate dendritic growth models has become vital at lower bulk temperatures. In addition to the thermal diffusion, the interface kinetics and curvature effects become non-negligible at such low temperatures and thus should be taken into account. In this study, we present a novel crystal growth model coupled with a heterogeneous nucleation model to investigate the dynamics of a recalescence stage during droplet freezing. A statistical framework is developed for the sensitivity analysis that uses the Monte-Carlo method to quantify the influence of self-diffusivity and the interface kinetic factor on the crystal growth rate, rigorously. Further, the model parameters are optimized using the minimization of the sum of the least-squares method. The proposed crystal growth model along with the optimized parameters can reliably simulate linear and nonlinear interface kinetics for metastable water of supercooling up to 30 K. Our key findings demonstrate that the dendritic growth rate is a strong function of the type of diffusivity expression, diffusivity parameters, and the interface kinetics factor. These findings can accurately capture the recalescence dynamics for the droplet freezing of pure Lennard-Jones liquids and, thus, would be of importance to several physicochemical, biological, and engineering applications.



## INTRODUCTION

Crystallization of a supercooled water droplet has been a topic of numerous scientific and experimental investigations. This is partly due to its widespread applications in several interesting and important physical,<sup>1–3</sup> biological,<sup>4–6</sup> and industrial occurrences;<sup>7–10</sup> and partly because of the complicated chemistry and physics involving supercooled water and ice formation. The combination of significance, complexity, and mystery associated with freezing of water renders this problem a holy grail for modern scientific and engineering pursuits. Droplet freezing has been demonstrated to be a multistage and multiscale phase-change problem.<sup>3,11,12</sup> Each stage of the freezing process is thermodynamically interlinked. The freezing starts with the nucleation of a supercooled droplet, which is followed by the rapid crystal growth stage. The stages of nucleation and crystal growth are also collectively known as the recalescence stage.<sup>11</sup> The recalescence stage is followed by an equilibrium freezing stage where the phase-change process is controlled by the type of boundary condition at the droplet surface.<sup>3,13</sup> After solidification, the solid subcooling stage causes the temperature of the solidified droplet to lower further until the droplet is in thermal equilibrium with the surroundings.<sup>3,13,14</sup> The recalescence stage plays a critical role in ascertaining the morphology of the crystal formed, its growth rate, and thermodynamics of the freezing process. Even though

the recalescence stage has been a subject of experimental, theoretical, and numerical studies since the early 20th century,<sup>11,15–19</sup> it still has numerous open research avenues in terms of different physical, electrical, and kinetic phenomena that govern the process of crystal growth.<sup>11,19–23</sup> During the recalescence stage, both the morphology and growth rate have been demonstrated to be a strong function of a solid–liquid interface temperature and humidity in the surrounding medium.<sup>24</sup> The morphological classification is broadly illustrated in the literature as Nakaya diagrams, which characterize the crystal shapes in the temperature and humidity space. According to a recent review by Libbrecht,<sup>25</sup> the physics behind this phenomena is not fully understood; however, a recent study by Jung et al.<sup>26</sup> postulates that the variability in environment humidity could lead to localized evaporation of the droplet. This could, in turn, impact the nucleation mechanism, and consequently, the crystal growth, the inclusion of which is

Received: December 7, 2020

Revised: April 20, 2021

demonstrated to improve the accuracy of predicting the freezing behavior (Gai et al.<sup>27</sup>). Several studies in the literature theorize that the crystal grows in the form of dendrites, a branching structure, in a metastable, supercooled, or supersaturated liquid.<sup>28–30</sup> The crystal growth rate, however, is complicated and needs a comprehensive theoretical treatment. Several experimental and theoretical attempts have been undertaken in the literature to study the thermophysical and kinetic dependencies of the crystal growth rate. Earlier attempts assumed the growth rate to be a power-law-type function of bulk supercooling and developed different empirical correlations that quantified the experimental growth rates well.<sup>15,31</sup> A summary of these studies is presented by Cahn et al.,<sup>31</sup> where they tabulated different growth velocity expressions of the form,  $v = \alpha \Delta T^\gamma$ , for different physical setups. The coefficients  $\alpha$  and  $\gamma$ , in this growth velocity expression, are empirically determined through curve fitting the experimental data. While these expressions are useful to quantify the growth rate under certain conditions, their accuracy and applicability is hardly universal and yields limited physical insights into the crystal growth process. The initial attempts to theoretically model dendritic growth from first-principles is often credited to Papapetrou.<sup>32</sup> He solved for the growth rate for a dendrite with a cylindrical tip surrounded by a steady-state thermal field. The assumption of cylindrical shape for a dendrite, however, was in contradiction with the experimental observations that showed the tip to be rather parabolic.<sup>28</sup> Ivantsov<sup>33</sup> solved the dendritic growth as a complex Stefan problem, which yielded a parabolic shape for the steady-state dendritic growth tip. Nevertheless, his solution was valid for a family of values for the dendritic growth rate and the curvature radius. To tackle this issue, a series of studies in the 70s and 80s came out,<sup>34–37</sup> with the goal of obtaining a unique, universal solution for the growth rate based on the stability criteria for dendrites. The famous LM-K stability theory<sup>34,35</sup> was an important landmark, which yielded a universal model of the growth rate as a function of bulk supercooling. The LM-K model, however, did not include the kinetic or curvature effects in its formulation and thus is valid only for a restrictive range of bulk supercooling. This issue was brought to light almost a decade and a half later by Shibkov et al.<sup>38,39</sup> who postulated that for higher values of bulk supercooling surrounding the crystal, the crystal growth mechanism faces a “cross-over” from a diffusion-controlled to a kinetic-controlled regime. Hence, at higher supercooling, the kinetic effects on dendritic growth cannot be neglected. Two pervasive theories in the literature to incorporate the kinetic effects within the dendritic growth rate framework are linear kinetic theory<sup>36,40</sup> and the Wilson–Frenkel model.<sup>16,17,29</sup> While both theories consider the effect of attachment kinetics in their formulation, the Wilson–Frenkel model has been demonstrated to predict the growth rates well for liquids with Lennard-Jones potential such as water.<sup>19,40</sup> The Wilson–Frenkel theory posits that the atomic diffusion process controls the net rate of attachment of molecules from supercooled liquid to a solid crystal structure which, in turn, determines the dendritic growth rate. Self-diffusivity and the interface kinetic parameter play a critical role in governing the accuracy of the Wilson–Frenkel model. These parameters, however, are difficult to measure experimentally. For instance, the interface kinetics factor,  $\beta$ , is a critical atomic-scale length in the Wilson–Frenkel model that is a function of the molecular volume, the fraction of interface sites that are also step sites, and the average diffusion jump distance, parameters which have not been reliably measured in a lab setting yet.<sup>41</sup> Similarly, while

recent studies have come a long way in measuring the self-diffusivity using experimental methods, there is still a non-negligible uncertainty that exists,<sup>42–44</sup> which, to the best of our knowledge, has not been taken into account toward crystal growth rate modeling in the literature. Owing to this uncertainty, no accepted values exist for these parameters to accurately measure the dendritic growth rate in a kinetic-controlled regime. The research question that begets from the aforesaid issues is threefold and is posed as follows:

- (i) What thermophysical properties, boundary conditions, and kinetic parameters affect the dendritic growth rate the most?
- (ii) How can we quantify the importance of each parameter?
- (iii) Could an optimization framework be formulated that can minimize the model error and increase its range of applicability in terms of the undercooling degree at the same time?

Motivated by these overarching research questions, this study formulates a rigorous statistical-cum-theoretical framework to incorporate the reported uncertainties of the thermophysical and kinetic variables while computing the dendritic growth rate of the undercooled water. The study commences by developing a heterogeneous nucleation model, which includes a relatively accurate form of a pre-exponential factor for nucleation in spherical particles, as recently formulated by Vehkamäki.<sup>45</sup> The nucleation model predicts the undercooling degree of the melt, which is an important consideration in the dendritic growth model to yield a holistic representation of the recalescence stage. Monte-Carlo simulations are then performed to quantify the sensitivity of important thermophysical and kinetic parameters on the dendritic growth rate. To incorporate the effect of thermal diffusion, interface kinetics, and curvature, the study devises a unique crystal growth model that considers all three undercooling mechanisms in estimating the dendritic growth rate. Due to their amplified effects at higher supercooling, interface kinetic models have been thoroughly examined. In addition to optimizing the Wilson–Frenkel model parameters for interface kinetics, the study also estimated the optimized value of the linear interface kinetics coefficient,  $\mu$ , for water solidification. The optimized diffusivity and kinetic parameters are then used to compare different variants of the Wilson–Frenkel model and investigate the effect of the curvature at higher undercoolings. The structure of the paper is as follows. First, in the **Methodology** section, we present the nucleation model, the crystal growth model, and the statistical framework. The crystal growth model description includes several prevalent approaches to estimate the thermal diffusion (Ivantsov’s model and LM-K theory), interface kinetics (Wilson–Frenkel and the linear model), and curvature effects (Gibbs–Thomson). The statistical subsection includes a detailed description of the sensitivity analysis and parametric estimation of different thermophysical and kinetic parameters in the Wilson–Frenkel model. The **Methodology** section is succeeded by the **Results and Discussion** section, which expounds upon the results of the sensitivity and optimization analysis of Wilson–Frenkel and linear kinetics undercooling models. It also discusses different variants of the Wilson–Frenkel model commonly used in the literature and the effect of the curvature on the dendritic growth velocity. Lastly, the paper culminates by summarizing the key findings of the study in the **Conclusions** section.

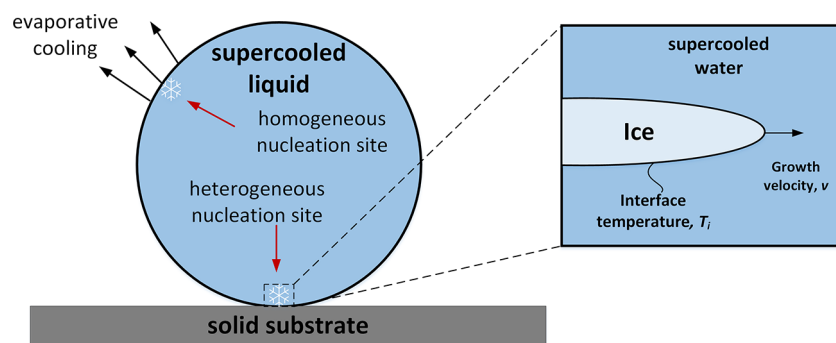


**Figure 1.** Sessile droplet freezing on a substrate. The inset shows the growth of a platelet-type dendrite.

## METHODOLOGY

This section presents the thermodynamic and kinetics model of nucleation and dendritic growth rate in a supercooled sessile droplet on a substrate. Moreover, it also outlines the statistical methodology for sensitivity analysis and parametric estimation, which form an important foundation for analyzing the key dependencies of the crystal growth model on thermophysical and kinetics parameters. For clarity, it is important to specify the definitions of commonly used terms throughout the manuscript here. The terms supercooling and undercooling are used interchangeably in the manuscript with both referring to the phenomena of water preserving its liquid phase even when it is cooled below the freezing point. Additionally, the supercooling degree or the undercooling degree refers to the temperature difference between the supercooled melt and the freezing temperature. Finally, the terms dendritic growth rate and dendritic growth velocity express the same phenomena of crystal growth velocity in the supercooled droplet.

Figure 1 illustrates the configuration of the sessile droplet examined in this study. The inset shows the growth of a platelet-type dendrite, which is a common morphology for a dendrite propagating in a supercooled medium for high supercooling.<sup>38</sup> The phenomenon of supercooling is necessary for many configurations to overcome the free-energy barrier posed by the phase-change process. For a supercooled droplet, nucleation can occur in different modes, which are broadly categorized into homogeneous and heterogeneous nucleation. In addition to the degree of supercooling, the occurrence of these modes is dependent on variables such as the cooling rate, surface morphology, wettability, relative humidity, shear flow, etc.<sup>23,26,46</sup> To simplify the subsequent analysis, this study assumes conditions that discourage localized supercooling on the outer surface of the droplet since it may engender formation of multiple nuclei. Thus, the mode of nucleation assumed in this study is heterogeneous nucleation at the contact surface. Nucleation is followed by dendritic growth, which, in the case of the supercooled water, is governed by different mechanisms of interfacial undercooling such as thermal, kinetic, and curvature based (Gibbs–Thomson effect).<sup>29</sup> There have been several models presented in the literature that have attempted to predict the crystal growth rate as a function of bulk supercooling. However, a majority of these models are limited in their range of applicability with regards to the supercooling degree. Here, we attempt to bridge the nucleation and the crystal growth model to gain physical insights into the two important stages of freezing. A sensitivity analysis and parametric estimation is also conducted to incorporate the reported variability in modeling approaches of kinetic undercooling and experimental measurements of

thermophysical/kinetic properties. The methodology presented in this section follows the subsequent steps:

- (1) First, a heterogeneous model based on classical nucleation theory (CNT) is developed.
- (2) The nucleation temperature calculated using the CNT is considered to be the bulk supercooling for the dendritic growth model.
- (3) Mathematical and physical models of different undercooling mechanisms affecting the dendritic growth rate and interface undercooling are presented.
- (4) Modified forms of two widely accepted theories to model kinetic undercooling, i.e., the Wilson–Frenkel model<sup>17</sup> and the linear interface kinetics model,<sup>47</sup> are formulated in combination with the thermal and curvature undercooling.
- (5) Different variants of the Wilson–Frenkel model and water’s self-diffusivities to be analyzed in the context of ice growth are presented.
- (6) The methodology for the sensitivity analysis of thermophysical and kinetic parameters on the crystal growth rate and interface temperature is posed.
- (7) Lastly, the statistical model of the parametric estimation to yield an optimized solution is outlined.

**Heterogeneous Nucleation Model.** For the process of phase change to occur, it is imperative that the free-energy barrier associated with the thermodynamics of phase change be surmounted. Phase change can either be brought about by the process of supersaturation (change in pressure) or supercooling (change in temperature). This study assumes that the droplet is kept at a constant, atmospheric pressure and thus supercooling is the only viable pathway for phase change. Supercooling in a water droplet is governed by the transient heat conduction equation subjected to a convective boundary condition.<sup>11,13</sup> The dimensionless governing equation is given by

$$\frac{\partial \Theta}{\partial \tau} = \frac{\partial^2 \Theta}{\partial \eta^2} + \frac{2}{\eta} \frac{\partial \Theta}{\partial \eta} \quad (1)$$

subjected to the boundary conditions

$$\left. \frac{\partial \Theta}{\partial \eta} \right|_{(1, \tau)} = -\text{Bi} \Theta(1, \tau)$$

$$\left. \frac{\partial \Theta}{\partial \eta} \right|_{(0, \tau)} = 0 \quad (2)$$

and the initial condition

$$\Theta(\eta, 0) = 1 \quad (3)$$

In eqs 1–3,  $\Theta_1 = (T - T_\infty)/(T_{\text{init}} - T_\infty)$  is the dimensionless temperature profile in the supercooled droplet,  $\eta = r/a$  is the dimensionless radial coordinate, and  $\tau$  is Fourier number given by  $\tau\alpha_1/a^2$ , where  $a$  is the radius of the droplet and  $\alpha_1$  is the thermal diffusivity of the supercooled liquid. The solution to eqs 1–3 can be obtained analytically and is given as<sup>48</sup>

$$\Theta_1 = \sum_{n=1}^{\infty} A_n e^{-\beta_n^2 \tau} f_n(\beta_n, \eta)$$

$$A_n(\beta_n) = \frac{2(\sin \beta_n - \beta_n \cos \beta_n)}{\beta_n - \sin \beta_n \cos \beta_n}$$

$$f_n(\beta_n, \eta) = \frac{\sin(\beta_n \eta)}{\beta_n \eta} \quad (4)$$

where  $\beta_n$  are the eigenvalues of the solution, which are governed by the expression,  $\beta \cos \beta + (\text{Bi} - 1)\sin \beta = 0$ .

While the solution provided by eq 4 takes into account the effect of boundary conditions and bulk thermophysical properties on the supercooling rate, a thermodynamic analysis at the atomic scale is necessary to evaluate the time and temperature at which it will be energetically favorable for the ice nucleus to form. CNT has proven to be useful in this regard because of its simplicity, practicality, and wide range of applicability. For the CNT to be applicable for the case of predicting the heterogeneous nucleation rate, the following assumptions are undertaken:

- (1) Nuclei is considered to be spherical in shape (geometric factor is unity).
- (2) Capillarity approximation is assumed to hold true for the ice nuclei.
- (3) State properties of the nuclei (temperature and pressure) are taken to be the same as the stable, supercooled, liquid phase.
- (4) A sharp interface is assumed between the nuclei and the supercooled water.
- (5) State and thermophysical properties within the nuclei are considered as isotropic and are assumed to be spatially uniform.
- (6) To ensure the formation of a single nucleus only, a low cooling rate is assumed.
- (7) Effect of humidity is not considered. The droplet is assumed to be surrounded by a dry medium to ensure no localized supercooling occurs on the outer droplet due to evaporation.

Following the analysis outlined by Hobbs<sup>49</sup> in his book, which is more recently extended by Meng et al.<sup>11</sup> and Tanaka et al.<sup>50</sup> to the supercooled water droplet, the nucleation rate for the formation of ice nuclei is derived as

$$J = D(T) \frac{A_m}{3} n_1^{7/3} \sqrt{\frac{A_m \sigma_{\text{is}}}{\pi k T}} \sqrt{\frac{4}{2 + \zeta_f}} \exp\left(\frac{16\pi \sigma_{\text{is}}^3 f(\theta)}{3[n_s \Delta\mu_{\text{is}}]^2 k_B T}\right) \quad (5)$$

In eq 5,  $D(T)$ <sup>42</sup> is the self-diffusivity of the supercooled water,  $n_{1/s}$  is the number density of water molecules of the liquid/ice particles,  $A_m$  is the surface area of a single water molecule,  $\sigma_{\text{is}}$ <sup>51</sup> is the interfacial surface tension,  $f(\theta)$ <sup>11</sup> is the heterogeneous free-energy factor,  $k_B$  is the Boltzmann constant, and  $T$  is the supercooled temperature governed by eq 4.  $\zeta_f$  is the

heterogeneous Zeldovich factor and is taken from Vehkamäki et al.<sup>45</sup> It is given by the expression

$$\zeta_f = \frac{(1 - X \cos \theta)[2 - 4X \cos \theta - (X^2 \cos^2 \theta - 3)]}{(1 - 2X \cos \theta + X^2)^{3/2}} \quad (6)$$

where  $X$  is the ratio between the radius of a nucleating particle and the radius of a critical embryo, and  $\theta$  is the contact angle between the droplet and the surface.  $\Delta\mu_{\text{is}}$ , also known as the thermodynamic driving force, is the difference in chemical potential between the supercooled liquid and ice. With the ideal gas approximation for water vapor, it can be expressed as

$$\Delta\mu_{\text{is}} = k_B T \log\left(\frac{p_w}{p_i}\right) \quad (7)$$

where  $p_w$  and  $p_i$  are the saturated liquid and ice pressures. For current study, the expressions for the saturated pressures are taken from Murphy and Koop.<sup>52</sup>  $f(\theta)$  in eq 5 takes into account the effect of a nucleating surface on the free-energy barrier to form the critical nuclei. It is given by

$$f(\theta) = \frac{(2 + \cos \theta)(1 - \cos \theta)}{4} \quad (8)$$

Equations 5–8 are used to compute the heterogeneous nucleation rate, which ultimately govern the nucleation time and temperature. Values of the thermophysical properties, atomic properties, droplet radius, and other boundary conditions used by this study are provided in Table 1. For low cooling rates, the nucleation temperature,  $T_{\text{nv}}$ , is defined as the temperature at which the critical nuclei  $N_v$  reaches 1.<sup>50</sup>  $N_v$  is calculated by the equation

**Table 1. Molecular Constants, Thermophysical Properties of Water and Ice, and Boundary Conditions for the Heterogeneous Nucleation Model**

property/constant	expression/value
density of water, $\rho_l$ [kg/m <sup>3</sup> ]	999.8
thermal conductivity of water, $k_l$ [W/(m·K)]	0.555
specific heat of water, $c_{p,l}$ [J/(kg·K)]	4200
density of ice, $\rho_s$ [kg/m <sup>3</sup> ]	916.2
thermal conductivity of ice, $k_s$ [W/(m·K)]	2.22
specific heat of ice, $c_{p,s}$ [J/(kg·K)]	2100
molecular weight, $M_w$ [g/mol]	18.05
interfacial surface tension, <sup>51</sup> $\sigma_{\text{is}}$ [J/m <sup>2</sup> ]	$0.025 + (T_i - 273.15) 10^{-4}$
self-diffusivity, <sup>42</sup> (VTF form) $D$ [m <sup>2</sup> /s]	$4 \times 10^{-8} \exp[-371/(T_i - 169.7)]$
latent heat of fusion, $L$ [J/kg]	334 000
Avogadro's constant, $N_a$ [1/mol]	$6.022 \times 10^{23}$
Boltzmann constant, $k_B$ [J/K]	$1.38064 \times 10^{-23}$
radius of nucleating particle, <sup>45</sup> $R_p$ [m]	$25.4 \times 10^{-6}$
molar latent heat, $L_{\text{mol}}$ [J/mol]	6020
LM-K stability constant, <sup>34</sup> $\sigma$ [–]	0.0253
capillarity length of water, <sup>34</sup> $d_0$ [m]	$2.88 \times 10^{-8}$
radius of water droplet, <sup>19</sup> $r$ [mm]	2–3.3
heat transfer coefficient, <sup>13</sup> $h$ [W/(m·K)]	200
equilibrium freezing temperature, $T_f$ [K]	273.15
ambient air temperature, $T_\infty$ [K]	243.15
contact angle, $\theta$ [deg]	90–150

$$N_v = \int_0^t (V_0 - V_c) J d\tilde{t} \quad (9)$$

where  $V_0$  is the initial droplet size and  $V_c$  is the size of the crystalline nucleus. Equation 9 is coupled with the supercooling temperature via eq 4. Nucleation time is defined as the time taken by the supercooled liquid to reach the nucleation temperature. Using the heterogeneous nucleation modeling approach outlined by eqs 1–9, nucleation times and temperatures are calculated for three different types of surfaces i.e., hydrophilic, hydrophobic, and superhydrophobic. The model presented here can be beneficial for designing an experimental setup with a controlled nucleation delay for crystal growth investigation.

**Crystal Growth Model.** After nucleation, the crystalline structure grows rapidly into the supercooled droplet. Crystal growth can be imagined to constitute a process whereby the neighboring atoms or molecules stack themselves together at kinks in steps on thermodynamically favorable sites.<sup>53</sup> The morphology and the rate of growth of the crystals propagating in this phase of freezing have been observed to be a strong function of the supercooling degree.<sup>15,25,38</sup> Shibkov et al.<sup>38</sup> experimentally measured the dendritic velocity while developing a morphology spectrum for different types of freely growing ice crystal morphology. While there is a wealth of literature on modeling the rate of dendritic growth for smaller supercooling of water in the thermal diffusion regime ( $\Delta T < 5^\circ\text{C}$ ),<sup>39</sup> attempts to compute the growth rates for higher supercooling are rather limited. This can be attributed to the domination of interface kinetics and curvature effects at higher supercooling, thus rendering the classical approach to describe dendritic growth limited in its scope. The classical model for dendritic growth from the pure melt is based on a diffusion-controlled moving boundary problem. The motion of the boundary, and consequently the crystal growth velocity, is dependent on the local temperature gradients and latent heat of fusion. The idea was pioneered by Papapetrou<sup>32</sup> and later formalized by Ivantsov.<sup>33</sup> The literature<sup>19,29,39</sup> shows, however, that the kinetic and curvature effects start dominating the dendritic morphology and growth rate for supercooling greater than 4–5 °C. This study includes the effects of thermal diffusion, interface kinetics, and curvature to model the growth rate and interfacial undercooling to incorporate a wider supercooling range. Thus, the total undercooling can be written as

$$T_f - T_n = \Delta T_h + \Delta T_k + \Delta T_c \quad (10)$$

where  $\Delta T_h$ ,  $\Delta T_k$ , and  $\Delta T_c$  are diffusive, kinetic, and curvature undercoolings of the interface, respectively. The left-hand side of eq 10 depicts the total undercooling of the melt at the nucleation temperature,  $T_n$ , with respect to the equilibrium freezing temperature,  $T_f$ . Whereas, the right-hand side quantifies the relative contribution of different mechanisms toward the total undercooling.  $\Delta T_h$  quantifies the thermal diffusion effects,  $\Delta T_k = T_i - T_f$  represents the kinetic undercooling, and  $\Delta T_c$  accounts for the curvature undercooling. The following subsections outline the thermophysical and kinetic models that quantify these contributions and relate these respective undercoolings to the crystal growth rate.

**Thermal Undercooling.** Assuming a cylindrically symmetric, isothermal, and paraboloid needle crystal, Ivantsov<sup>33</sup> solved the heat diffusion equation coupled with the moving boundary problem, which yielded a family of solutions for parabolic crystallization front. His solution, however, ignored capillarity

and kinetic effects. His solution for the thermal undercooling,  $\Delta T_h$ , as a function of growth velocity,  $v$ , and Peclet number  $Pe = vR/2\alpha_s$  can be written as

$$\frac{c_p \Delta T_h}{L} = \text{Iv}(Pe), \quad \text{Iv}(Pe) = Pe \exp(Pe) E_1(Pe) \quad (11)$$

where  $R$  is the tip radius of the paraboloid,  $c_p$  is the specific heat of liquid water,  $L$  is the latent heat of fusion, and  $\alpha_s$  is the thermal diffusivity of undercooled water.  $E_1(Pe)$ , in eq 11 is the exponential integral and  $\Delta T_h$ , i.e., the initial supercooling of the melt in the absence of kinetic and curvature effects, equals  $T_f - T_n$ .

The solution given in eq 11 is not unique. Rather, it yields the product,  $vR$ , which holds true for several values of the tip radius and dendritic growth velocities. Experimental evidence, however, points toward the assertion that for a given supercooling, a unique solution for  $v$  and  $R$  exists. This begets establishing selection criteria that can yield an accurate solution. To tackle this, Langer and Müller-Krumbhaar<sup>34</sup> put forward the principle of a marginal stability criterion for the tip radius selection. In the literature, it is also commonly known as the LM-K model. They posited that the unique dendrite bifurcates the stable and unstable regions determined by a universal selection parameter,  $\sigma$ , which was defined as  $\sigma = (\lambda_s/2\pi R)^2$ .  $\lambda_s$  is the Mullins–Sekerka stability length that further takes into account the side branching instability of the dendrites and is given by  $\lambda_s = 2\pi\sqrt{2\alpha_s d_0/v}$  where  $d_0$  is the capillarity length. Equating the tip radius,  $R$ , with the stability length,  $\lambda_s$ , and combining the expressions for  $Pe$ ,  $\sigma$ , and  $\lambda_s$ , we get the following relations

$$v = \frac{2\alpha_s \sigma}{d_0} Pe^2, \quad \sigma = \frac{1}{4\pi^2} \quad (12)$$

Equation 11 in conjunction with eq 12 constitutes the solution of the LM-K model for dendritic growth. While the model has been successfully demonstrated to predict crystal growth rates in water, succinonitrile, and camphene for low supercooling, it significantly overpredicts  $v$  for supercooling greater than  $\sim 4^\circ\text{C}$ . This calls for the inclusion of a kinetic undercooling term within the thermodynamic framework to factor in the interface kinetic effects at higher supercooling.

**Kinetic Undercooling.** Equations 11 and 12 are based on the assumption that the interface between the crystal and liquid is at the equilibrium freezing temperature,  $T_f$ . For higher undercoolings with non-negligible interface kinetic effects, the interface temperature,  $T_i$ , however is supercooled to a temperature lower than  $T_f$ . The extent to which the interface is supercooled from  $T_f$  due to kinetic effects is referred as kinetic undercooling, which equals  $\Delta T_k = T_f - T_i$ .

To incorporate the interface kinetics, the expression of the growth rate for crystal needs to be revisited and re-expressed as a function of  $T_i$ . There are two common approaches to this presented in the literature, both of which are explored in our study. The simplified, linear kinetic models assumes  $\Delta T_k$  to be directly proportional to the crystal growth velocity,  $v$ . The constant of proportionality, in this case, is termed as the linear kinetic coefficient,  $\mu$ .<sup>19,36,54</sup> Substituting  $\Delta T_k = v/\mu$  in eq 10, along with the values of  $\Delta T_h$  and  $\Delta T_c$  from eqs 11 and 22, we get the following

$$T_f - T_n = \frac{L}{c_p} \text{Iv}\left(\frac{vR}{2\alpha_s}\right) + v/\mu + \frac{\sigma_s T_f}{L_v} \sqrt{\frac{v\sigma}{2d_0\alpha_s}} \quad (13)$$

where the only unknown is the dendritic growth velocity,  $v$ . Equation 13 is an implicit, nonlinear equation and is solved using the bisection method in MATLAB software. In the literature,  $\mu$  has been used as a tuning parameter to get a good agreement between the experimental and numerical results for the crystal growth rate under different supercooling. Lipton et al.<sup>55</sup> used the linear interface kinetics model with thermal and solutal undercooling to estimate  $\mu$  for phosphorous. Yong-Jun et al.<sup>56</sup> used the same model to estimate the effect of interface kinetics on the dendritic growth rate of water droplets. The linear kinetics model, while simple and easy to implement, has some shortcomings. First, recent molecular dynamics simulations have shown that the kinetic coefficient,  $\mu$ , is anisotropic, i.e., its value varies along different crystal growth directions.<sup>40,57</sup> Second, the dendritic growth rates for liquids with Lennard-Jones potential such as water does not match well with the linear interface kinetics model.<sup>28</sup> Instead, the interface kinetics model proposed by Wilson<sup>17</sup> and later modified by Frenkel<sup>16</sup> is in better agreement with the experimental results. The model, referred to as the Wilson–Frenkel model, hereafter, attempts to link undercooled interface temperature  $T_i$  with  $v$  and estimates the rate at which liquid atoms or molecules join the crystal. This “jump” of the atoms or molecules across the phase is a strong function of the self-diffusion coefficient in the liquid,  $D$ , and the difference in chemical potential between the parent and new phase  $\Delta\mu_{ls}$ , both of which, in turn, are a strong function of  $T_i$ . The Wilson–Frenkel model estimates the growth velocity,  $v$ , as  $v = \sqrt[3]{\Omega w f u}$ , where  $\Omega$  is the atomic volume of water molecule,  $w$  is the rate of atoms joining the crystal at the repeatable step sites,  $f$  is the fraction of interface sites that are also the step sites, and  $u$  is the net rate of atoms arriving at the kink sites. With  $u$  rewritten as  $1 - \exp(-\Delta\mu_{ls}/k_B T_i)$  and  $w$  evaluated as  $w = \delta \exp(-Q/k_B T_i) \exp(-L/k_B T_i)$ , the crystal growth velocity becomes

$$v = f \sqrt[3]{\Omega} \delta \exp\left(\frac{-Q}{k_B T_i}\right) \exp\left(\frac{-L}{k_B T_i}\right) \left[1 - \exp\left(\frac{-\Delta\mu_{ls}}{k_B T_i}\right)\right] \quad (14)$$

where  $\delta$  is the frequency of the order of Debye frequency. The diffusion coefficient,  $D$ , can be further expressed as<sup>29</sup>  $D = (\Lambda^2 \delta / 6) \exp(-Q/k_B T_i)$ , where  $\Lambda$  is the average diffusion jump distance in the supercooled liquid. Expressing eq 14 in terms of  $D(T_i)$  yields

$$v = \frac{6D(T_i)}{\beta} \exp\left(\frac{-L}{k_B T_i}\right) \left[1 - \exp\left(\frac{-\Delta\mu_{ls}}{k_B T_i}\right)\right] \quad (15)$$

where  $\beta = \Lambda^2 / f \sqrt[3]{\Omega}$  is a length scale of the order of size of a molecule and is denoted as the interface kinetic factor in the literature.<sup>19,43</sup> Equation 15 is the general expression for the modified Wilson–Frenkel model. Several variants of this model are used in the literature, most of which differ because of the different underlying assumptions and modeling approaches taken to evaluate  $\Delta\mu_{ls}$ . Furthermore, the self-diffusion coefficient,  $D(T_i)$ , is also very critical to the accuracy of the crystal growth rate from the Wilson–Frenkel model. The current study explores the effect of three most commonly used variants of the Wilson–Frenkel model brought about by three different ways of approximating  $\Delta\mu_{ls}$ . The study also explores the relative accuracy of two commonly used empirical forms for self-diffusivity, i.e., Vogel–Tamman–Fulcher (VTF)<sup>42,43</sup> and the fractional power law (FPL),<sup>44,58</sup> on predicting the crystal growth rate. For small departures from the equilibrium state at constant pressure,  $\Delta\mu_{ls}$  can be rewritten in terms of the entropy change

during the phase-change process as  $\Delta\mu_{ls} = \Delta S_{ls}(T_f - T_i)$ . The change in the entropy for the system experiencing phase change at a molecular level is further given by  $\Delta S_{ls} = (L_{mol}/N_a)/T_f$ , where  $L_{mol}$  is the latent heat of fusion per unit mole and  $N_a$  is the Avagadro’s number. Incorporating these expressions in eq 15 and simplifying, we get the first variant of the Wilson–Frenkel model

$$v = \frac{6D(T_i)}{\beta} \left[ \exp\left(\frac{-L_{mol}}{\bar{R}T_m}\right) - \exp\left(\frac{-L_{mol}}{\bar{R}T_i}\right) \right] \quad (16)$$

where  $\bar{R} = k_B N_a$  is the universal gas constant. We can simplify eq 16 further by linear approximation of the term  $\exp(-\Delta\mu_{ls}/k_B T_i)$ . Using Taylor series expansion and linearizing, the second variant becomes

$$v = \frac{6D(T_i)}{\beta} \left[ \exp\left(\frac{-L_{mol}}{\bar{R}T_f}\right) \frac{L_{mol}(T_f - T_i)}{\bar{R}T_f T_i} \right] \quad (17)$$

Another way to model the change in chemical potential during phase change is using the ideal gas approximation for the water vapor.  $\Delta\mu_{ls}$ , in this case becomes,  $\Delta\mu_{ls} = k_B T_i \log p_l/p_s$ . Substituting this expression in eq 17, the third variant of the model is written as

$$v = \frac{6D(T_i)}{\beta} \exp\left(\frac{-L_{mol}}{\bar{R}T_f}\right) \left(1 - \frac{p_l}{p_s}\right) \quad (18)$$

where  $p_l$  and  $p_s$  are saturation pressures of supercooled liquid water and ice, respectively, and are a function of interface temperature,  $T_i$ . The expressions for  $p_l(T_i)$  and  $p_s(T_i)$  are taken from Murphy and Koop.<sup>52</sup> The accuracy of the variants listed in eqs 16–18 in conjunction with two commonly used empirical relations of diffusivities is explored in this study. For  $D(T_i)$  the Vogel–Tamman–Fulcher correlation is given by the equation

$$D(T_i) = D_0 \exp\left(-\frac{B}{T_i - T_0}\right) \quad (19)$$

where  $D_0$  and  $B$  are the fitting constants and  $T_0$  is the glass-transition temperature.  $B$ , in eq 19, is proportional to the activation energy of self-diffusivity for supercooled water. The Fractional Power Law fit for  $D(T_i)$  takes the form

$$D(T_i) = D_0 \sqrt{T_i} \left(\frac{T_i}{T_s} - 1\right)^\gamma \quad (20)$$

where  $D_0$  and  $\gamma$  are fit constants and  $T_s$  is the low-temperature threshold where  $D_0$  approaches zero.

**Curvature Undercooling.** The term  $\Delta T_c$  in eq 10 represents the contribution of the curvature of the interface to the total undercooling of the liquid–crystal interface. The phenomenon, commonly known in the literature as the Gibbs–Thomson effect, posits that at a low radius of curvatures, the melting point of the liquid tends to suppress itself. Rewriting eq 12 in terms of the radius of the interface curvature,  $R$ , and simplifying gives

$$R = \sqrt{\frac{2\alpha_s d_0}{v\sigma}} \quad (21)$$

Equation 21 shows that  $R$  would decrease with the increasing dendritic velocity, and by extension, increasing undercooling. Thus, it is important to include the effect of the curvature in the dendritic growth model at higher undercoolings. According to

Jackson,<sup>28</sup>  $\Delta T_c$  can be expressed as  $\Delta T_c = \frac{2\sigma_{ls}}{R\Delta S}$ , where  $\Delta S = L_v/T_f$  and  $R$  is given by eq 21. On substituting and simplifying we get

$$\Delta T_c = \frac{\sigma_{ls}T_f}{L_v} \sqrt{\frac{\nu\sigma}{2d_0\alpha_s}} \quad (22)$$

where  $L_v$  is latent heat per unit volume.

**Total Undercooling.** To compute the total supercooling as a function of growth velocity and interface temperature, eq 10 should be used. On substituting eqs 11 and 22 in eq 10 we get

$$T_f - T_n = \frac{L}{c_p} \text{Iv} \left( \frac{\nu R}{2\alpha_s} \right) + (T_i - T_f) + \frac{\sigma_{ls}T_f}{L_v} \sqrt{\frac{\nu\sigma}{2d_0\alpha_s}} \quad (23)$$

Equation 23 has two unknowns and should be used in conjunction with the interface kinetics model variants. Each of these variants given by eqs 16–18 should be solved simultaneously with eq 23 to yield  $\nu$  and  $T_i$  for different values of the supercooling degree (also referred as the nucleation temperature),  $T_n$ . Since these set of equations are nonlinear and implicit, they must be solved numerically to yield a meaningful and physical solution. This study implemented the bisection method in MATLAB software to solve the governing equations for  $\nu$  and  $T_i$ .

**Sensitivity Analysis and Parametric Estimation.** An analysis of eqs 23 and 15 shows that the self-diffusivity of water,  $D(T_i)$ , and the interface kinetics factor,  $\beta$ , are important variables of interests that critically determine the accuracy of our model for dendritic growth velocity,  $\nu$ , and interface temperature,  $T_i$ . However, some variability is reported in the literature for both  $\beta$  and  $D(T_i)$ . For instance, Xu et al.<sup>43</sup> computed the values of  $\beta$  to be  $1.33 \times 10^{-10}$  m for crystallization of water.<sup>a</sup> They calculated their  $\beta$  using their experimentally measured growth rate,  $\nu$ , and the VTF expression for  $D(T_i)$  from the empirical correlations by Price et al.<sup>42</sup> and Gillen et al.<sup>59</sup> Their measured crystal growth rate, however, does not agree well with the dendritic growth rates of water at higher supercooling, as measured by Shibkov et al.,<sup>38</sup> and, more recently, by Wang et al.<sup>19</sup> Using this observation, Wang et al.<sup>19</sup> used  $\beta$  as a tuning parameter and reported that the  $\beta$  value of  $6.2 \times 10^{-11}$  m minimized the sum of least-squared error between their model and experiments. Their model, however, did not take into account the curvature effects and variability of diffusivity parameters, such as  $B$ ,  $D_0$ , and  $T_0$ . This study takes the reported variability of the aforementioned parameters into consideration using the Monte-Carlo method. The effect of variability of kinetic and diffusivity parameters such as  $\beta$  (kinetic),  $B$ ,  $D_0$ ,  $\gamma$ ,  $T_s$ , and  $T_0$  (diffusivity—VTF and FPL forms)<sup>42,44</sup> on the output parameters of interests such as  $\nu$ , and  $T_i$  has been quantified using correlation coefficients. Figure 2 outlines the methodology used by this study to analyze the sensitivity of the aforementioned parameters on  $\nu$  and  $T_i$ .

The range of the model parameters used in this study is tabulated in Table 2. Uniform distribution is used for all of the model parameters while the latin hypercube method is employed to generate random samples. A sample size of 300 yielded no further variations in the correlation coefficients. Furthermore, the supercooled temperature for the sensitivity analysis is taken to be constant at 250 K. The temperature is chosen so that the system is representative of dendritic growth in the kinetic-controlled regime. The sample simulation space illustrating all of the simulation points used in this study to quantify the sensitivity is shown in Figure 3 for VTF and Figure 4

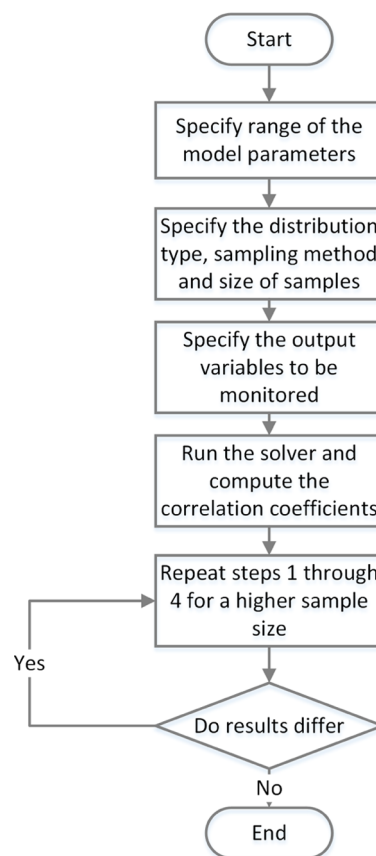


**Figure 2.** Flow chart for conducting the sensitivity analysis of diffusivity parameters and interface kinetic factor ( $\beta$ ) on dendritic growth velocity,  $\nu$ , and  $T_i$ .

**Table 2.** Range of the Kinetic and Diffusivity Parameters Used for the Sensitivity Analysis<sup>42,a</sup>

model parameter	minimum	average	maximum
Vogel–Tamman–Fulcher (VTF) Correlation [eq 19]			
$D_0$ <sup>42</sup> [m <sup>2</sup> /s]	$3.13 \times 10^{-8}$	$4 \times 10^{-8}$	$4.87 \times 10^{-8}$
$B$ <sup>42</sup> [K]	326	371	416
$T_0$ <sup>42</sup> [K]	163.6	169.7	175.8
$\beta$ <sup>19,43</sup> [m]	$6 \times 10^{-11}$	$1.3 \times 10^{-10}$	$2 \times 10^{-10}$
Fractional Power Law (FPL) Correlation [eq 20]			
$D_0$ <sup>42</sup> [m <sup>2</sup> /s]	$7.42 \times 10^{-8}$	$7.66 \times 10^{-8}$	$7.9 \times 10^{-8}$
$T_s$ <sup>42</sup> [K]	216.6	219.2	221.8
$\gamma$ <sup>42</sup> [m]	1.64	1.74	1.84
$\beta$ <sup>19,43</sup> [m]	$6 \times 10^{-11}$	$1.3 \times 10^{-10}$	$2 \times 10^{-10}$

<sup>a</sup>Undercooling temperature is assumed to be constant at 250 K for the sensitivity analysis.

for FPL correlation for the self-diffusivity. A Simulink model has been developed in MATLAB software that solves eqs 23 and 16 for 300 sample points both for the VTF and FPL diffusivity parameters, as given in eqs 19 and 20. Following the computation of the response variables for each of these simulation points, the statistical dependence of the model parameters and response variables are quantified using the Pearson's linear correlation, Spearman's rho correlation (also known as ranked correlation), standardized regression, and ranked standardized regression methods.<sup>60,61</sup> A discussion on the response variables and correlation coefficients for both the sample spaces is presented in the Results and Discussion section.

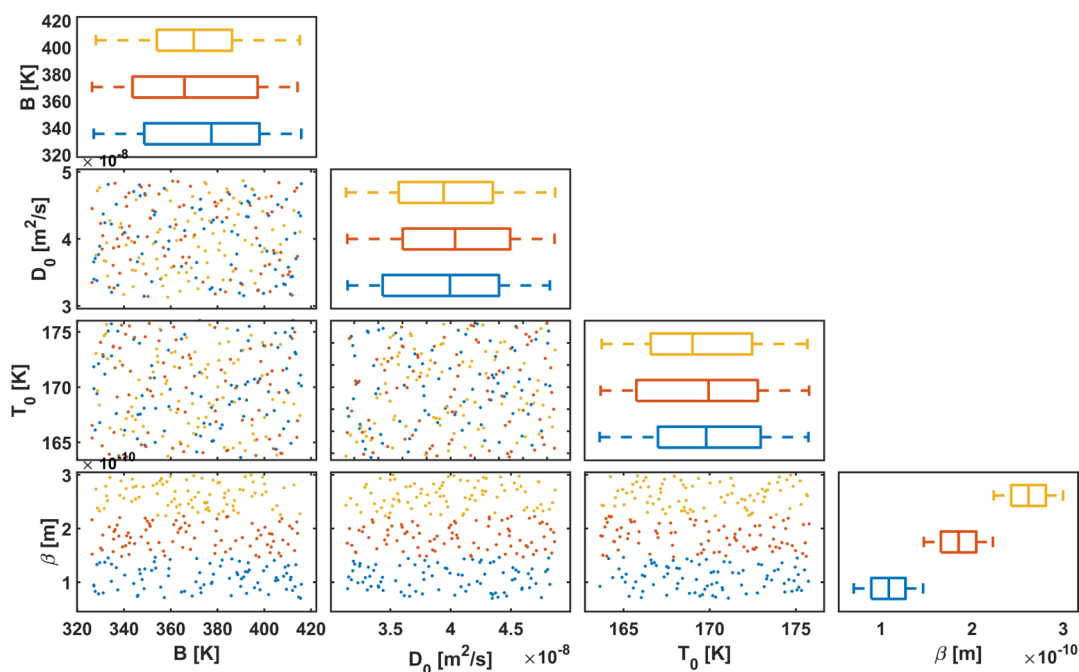


**Figure 3.** Sample space for the sensitivity analysis of the Wilson–Frenkel model using the VTF correlation for self-diffusivity. The colors blue, red, and yellow symbolize low, medium, and high levels of  $\beta$ , respectively.

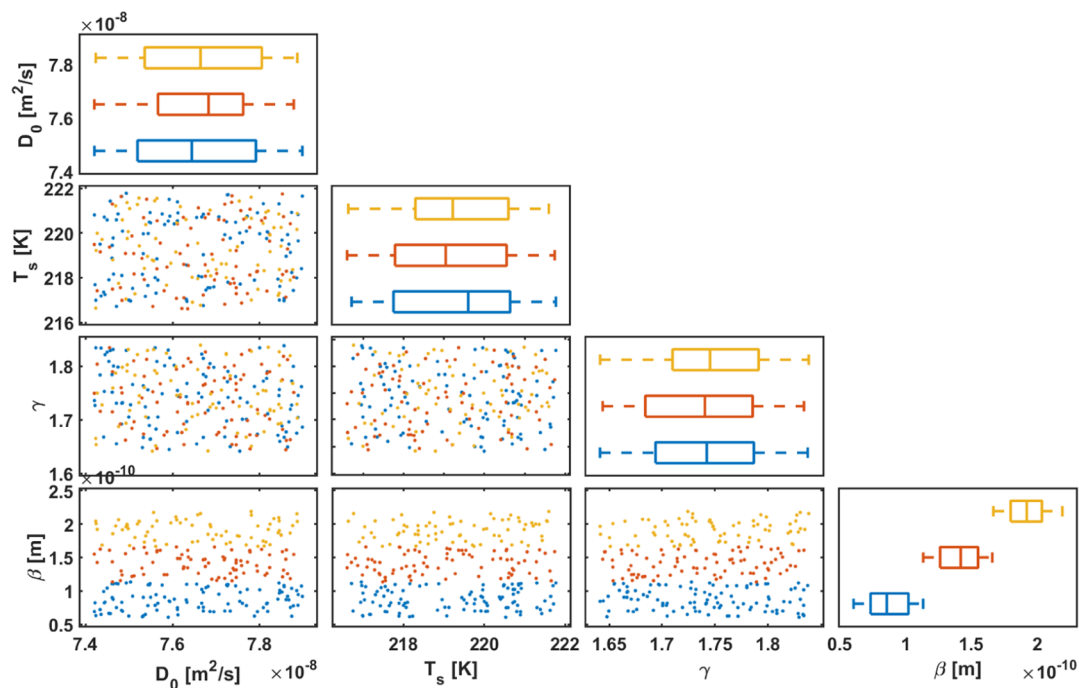


**Figure 4.** Sample space for the sensitivity analysis of the Wilson–Frenkel model using the FPL correlation for self-diffusivity. The colors blue, red, and yellow symbolize low, medium, and high levels of  $\beta$ , respectively.

After identifying the model parameters that are correlated strongly with the output variables, it is important to determine the accurate values of these parameters that reflect the experimental observation. To achieve that, we built an optimization function in MATLAB software that uses the sum of the squared difference between the simulated and experimental dendritic growth rates at different supercooling as the objective function and returns the optimized values of the model parameters that minimize the objective function. A gradient optimization algorithm is used to obtain the global

minima of the objective function. The details of the process are illustrated in Figure 5. To compute the objective function, it is important to have both simulation and experimental data. The study builds a simulation function based on the methodology outlined in the *Crystal Growth Model* section, whereas the experimental results are taken from the recent study by Wang et al.<sup>19</sup> The parametric estimation code has been developed in MATLAB software with the methodology outlined in Figure 5. After developing the objective function, the initial guess of the parameters along with the lower and upper bounds are specified.

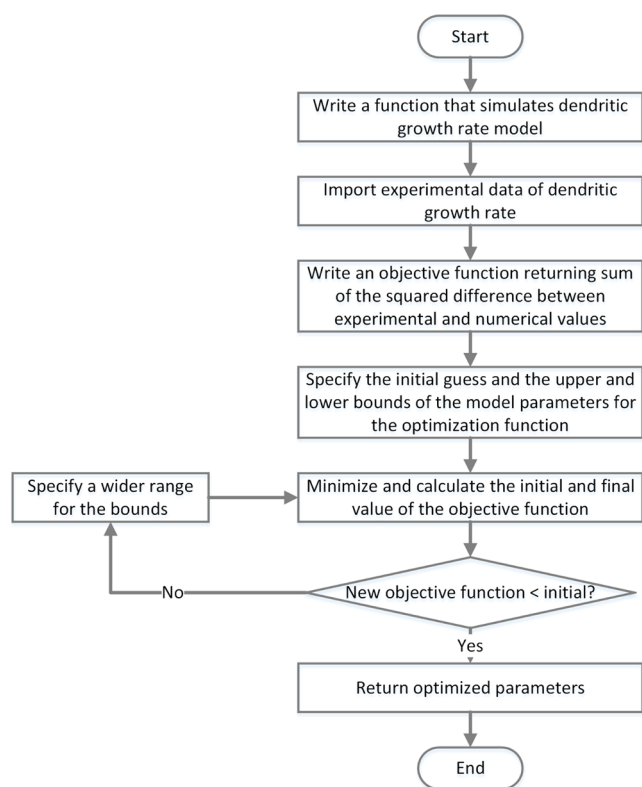


**Figure 5.** Flow chart for conducting the parametric estimation of diffusivity parameters and the interface kinetic factor ( $\beta$ ) using the sum of the least-squares method.

The code then computes the objective function within the specified bounds of model parameters and returns the parameter values that minimizes the objective function. For the Wilson–Frenkel model, both the kinetic and diffusivity parameters have been optimized, whereas for the linear kinetic model, an optimized linear kinetic coefficient of water has been obtained.

## RESULTS AND DISCUSSION

In this study, the nucleation times and temperatures for freezing water droplets of 5–15  $\mu\text{L}$  volume have been computed at different surface hydrophobicities. Furthermore, the results from the sensitivity and optimization analysis of Wilson–Frenkel and linear interface kinetics models for dendritic growth during the recalescence stage using the methodology outlined in the previous section are presented here. The effects of different variants of Wilson–Frenkel model formulation and curvature on the prediction of the dendritic growth rate,  $v$ , and interface temperature,  $T_i$  have also been discussed.

### Effect of Contact Angle on Nucleation Temperature.

Using the solution outlined in the heterogeneous nucleation model, the results for the nucleation time and temperature for three different diameters and contact angles are presented in Table 3. The nucleation model is validated with the experimental results of Hindmarsh et al.<sup>13</sup> for the water droplet of a radius,  $a = 0.78$  mm, subjected to convective cooling with the heat transfer coefficient,  $h = 180$  W/(m $\cdot$ K), and the free stream temperature,  $T_\infty = 258.15$  K. The nucleation time and temperature predicted by our model agree to be within 5% of the experimental data, thus affirming the accuracy of the model. Table 3 illustrates that the model correctly predicts the trend in the delay of nucleation with the increasing hydrophobicity of the

**Table 3.** Nucleation Times and Temperature of Freezing Water Droplets for Surfaces with Different Hydrophobicities

droplet volume, $V_d$ [ $\mu\text{L}$ ]	contact angle, $\theta$ [deg]	nucleation time, $t_n$ [s]	nucleation temp., $T_n$ [K]
5	90	10.5	254.35
	120	16.15	248.75
	150	19.55	246.75
10	90	13.8	254.35
	120	20.83	248.65
	150	25.15	246.65
15	90	16.3	254.35
	120	24.44	248.75
	150	29.4	246.65

substrate. This delay has been well documented by the previous studies<sup>22,46,62</sup> and can be attributed to the increase in the free energy required for the phase change to occur for low contact areas between the nucleating surface and the freezing droplet. The results from the validated nucleation model show that the nucleation time almost doubles for a superhydrophobic surface (contact angle 150°) as compared to the hydrophobic surface of a contact angle 90° for different droplet volumes. Further, an increase is also observed in the nucleation times for droplets with higher volumes. These results imply that to achieve longer nucleation delays for achieving controlled cooling rates in crystal growth experiments, superhydrophobicity and the droplet diameter play an important role. The model developed here can be used to predict the nucleation delay quantitatively, thus aiding in designing effective freezing experiments.

**Sensitivity Analysis and Optimization of Crystal Growth Models.** Diffusivity,  $D(T_i)$  and the interface kinetics factors,  $\beta$ , are identified to be the parameters of critical importance in our dendritic growth model. However, to the best of our knowledge, no universally accepted value or expression exists in the literature for them. The sensitivity analysis, as explained in the Methodology section, aims to answer the question: How can we quantify the relative importance of these parameters in the context of computing crystal growth velocity,  $v$ , and interface temperature,  $T_i$ ? Following the results of the sensitivity analysis, the next logical step is to identify the precise combination of the values of the parameters that strongly affect the crystal growth rate. The parametric estimation code using the sum of the least-squares method, as explained in the Methodology section, achieves exactly that. Here, we present the results of the sensitivity analysis of the two widely used self-diffusivity expressions in the literature, followed by the optimization of our model parameters.

Figure 6 shows the scatter plot of the response variables ( $v$ , and  $T_i$ ) as a function of diffusivity parameters of the VTF expression ( $B$ ,  $D_0$ , and  $T_0$ ) and the interface kinetic factor,  $\beta$ . The box plots on the right-hand side quantify the average values of  $v$  and  $T_i$  for different levels of  $\beta$  values in addition to the variability of these parameters. A quick analysis shows that  $\beta$  has an inverse effect on  $v$  and  $T_i$ . A similar inverse trend is also observed for the diffusivity coefficient,  $B$ , and the glass-transition temperature,  $T_0$ .  $D_0$ , however, directly affects the response variables. The average values of the response variables and their variability as depicted by the box plots also yield interesting insights. For low values of  $\beta$ , a wider spread of samples is observed for both  $v$  and  $T_i$  as signified by the longer box plots. However, as  $\beta$  increases, the variability in the response parameters decreases. This posits

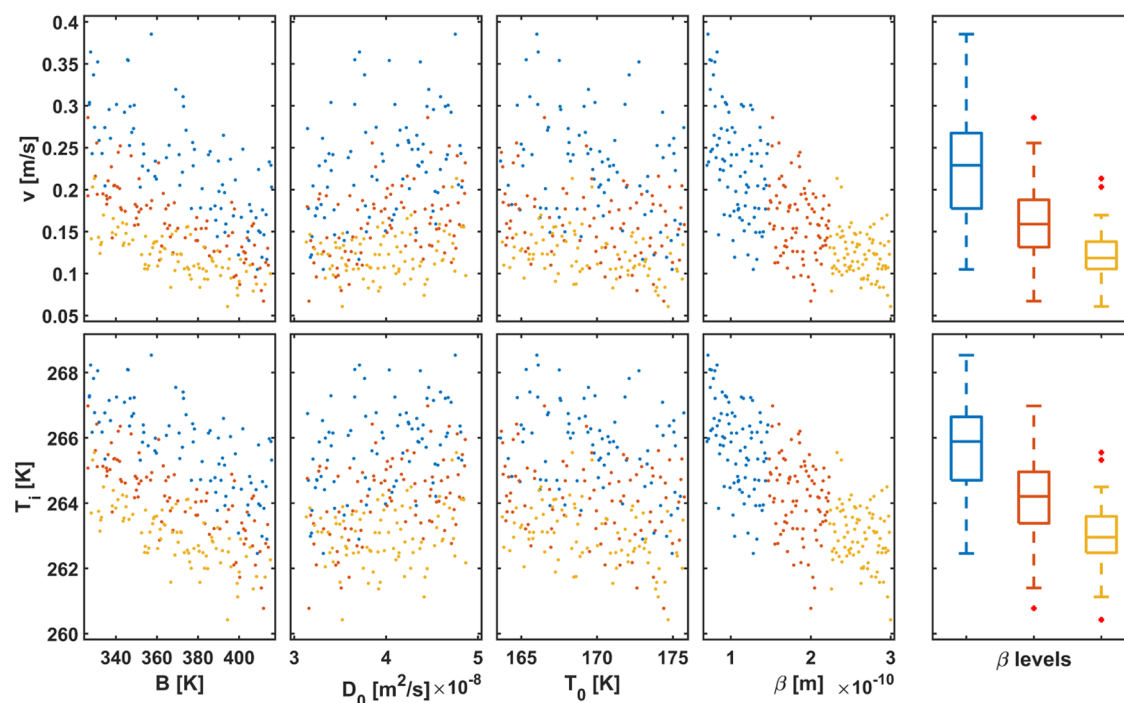


**Figure 6.** Velocity,  $v$ , and interface temperature,  $T_i$ , response for the 300 points in the simulation space shown in Figure 3 (VTF form). Colors blue, red, and yellow demonstrate low, medium, and high levels of the interface kinetic factor,  $\beta$ .

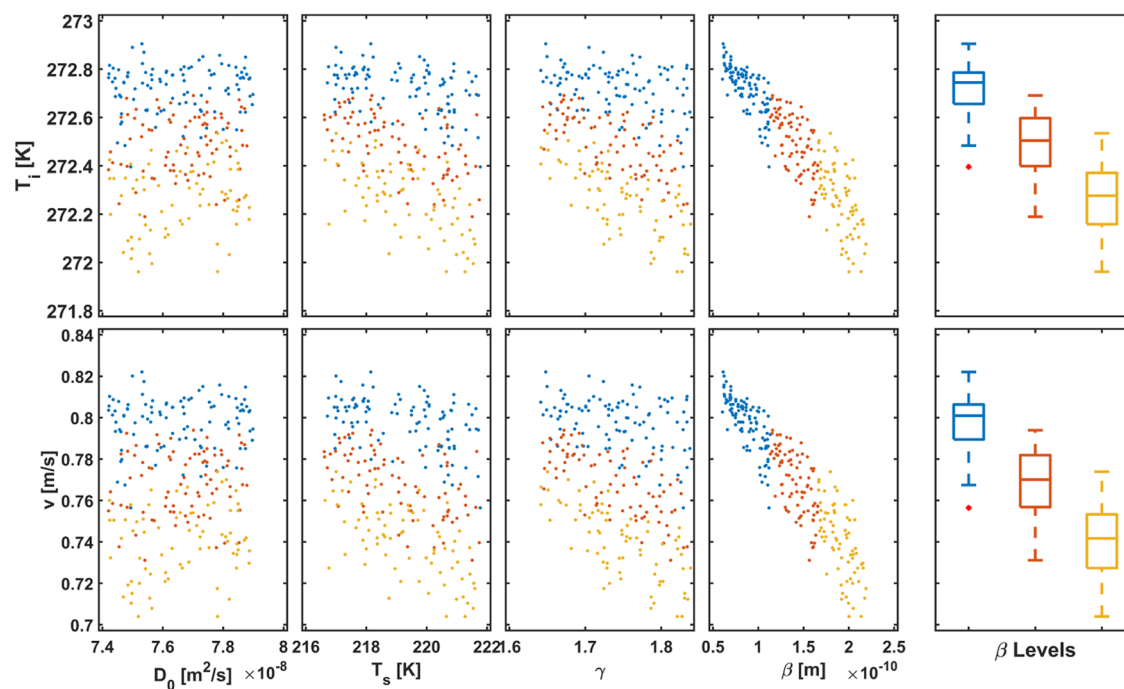


**Figure 7.** Velocity,  $v$ , and interface temperature,  $T_i$ , response for 300 points in the simulation space shown in Figure 4 (FPL form). Colors blue, red, and yellow demonstrate low, medium, and high levels of the interface kinetic factor,  $\beta$ .

that the solution is more sensitive to  $\beta$  values in the range of 0.6–1.5 Åm.

The response variables as a function of the FPL form of self-diffusivity and the kinetic parameter,  $\beta$ , are illustrated in Figure 7. From the scatter plots, it is evident that the response variables are not strongly correlated with the diffusivity parameters of the FPL form. However, a strong correlation is observed for the  $\beta$  values. This can be attributed to the fact that the reported variability in the model parameters for the FPL form of

diffusivity  $D_0$ ,  $\gamma$ , and  $T_s$  is lower as compared to the VTF form. This is also reflected in the range of the response parameters for FPL. For instance, the range of  $v$  for the FPL form (Figure 7) is reduced and lies between 0.7 and 0.83 m/s, whereas for the VTF form (Figure 6), it exhibits a wider range and stands between 0.05 and 0.38 m/s. A similar trend holds for  $T_i$  as well while comparing the two diffusivity forms.

Figures 6 and 7 qualitatively illustrate that the extent of the correlation of the response variables with each of the diffusive

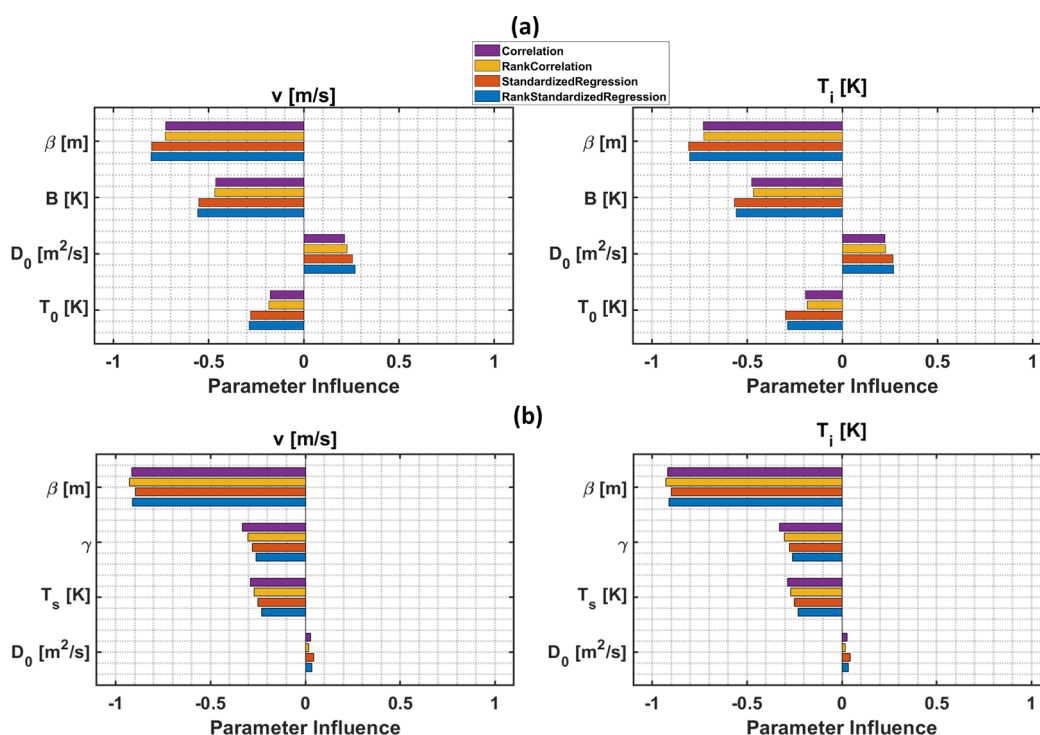


Figure 8. Tornado plots illustrating the influence of diffusivity and kinetic parameters on  $v$  and  $T_i$  for (a) VTF form and (b) FPL form.

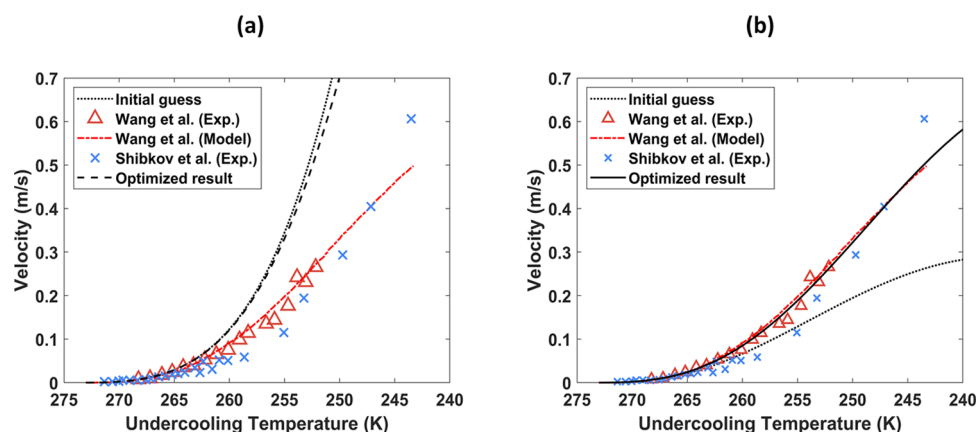


Figure 9. Optimized results for the two diffusivities form, (a) FPL and (b) VTF. Experimental data shown here are within the error margin of 6%. The values of initial guess of the parameters and the final optimized parameterized are tabulated in Table 4.

Table 4. Initial Guess Values and Optimized Values for VTF and FPL Diffusivity Parameters and the Interface Kinetic Factor,  $\beta$ , for the Crystal Growth Model

diffusivity correlation model					
Vogel–Tamman–Fulcher (VTF) correlation			fractional power law (FPL) correlation		
parameter	initial	optimized	parameter	initial	optimized
$\beta$ [m]	$1.3 \times 10^{-10}$	$5.47 \times 10^{-11}$	$\beta$ [m]	$1.3 \times 10^{-10}$	$2 \times 10^{-10}$
$D_0$ [ $\text{m}^2/\text{s}$ ]	$4 \times 10^{-8}$	$3.9 \times 10^{-8}$	$D_0$ [ $\text{m}^2/\text{s}$ ]	$7.66 \times 10^{-8}$	$7.42 \times 10^{-8}$
$B$ [K]	371	371	$\gamma$ [–]	1.74	1.84
$T_0$ [K]	169.7	169.7	$T_s$ [K]	219.2	220.8
obj. func.	0.91	0.13	obj. func.	3.78	3.53

and kinetic model parameters is different. This is more formally quantified through tornado plots of statistical correlations comparing different parameters and is mirrored in Figure 8 (a) for VTF correlation and (b) for FPL correlation. For both simulation scenarios, the parameter of critical influence turns

out to be the interface kinetics factor,  $\beta$ . This reaffirms the findings of the previous studies by Wang et al.,<sup>19</sup> Xu et al.,<sup>43</sup> and Jackson.<sup>29</sup> As for the diffusivity parameters, the results are dependent on the type of self-diffusivity correlation tested. For the FPL form, the self-diffusivity parameters do not seem to

impact  $v$  and  $T_i$  substantially, whereas for the VTF form, the fit parameter  $B$ , which is related to the activation energy of self-diffusion of water,<sup>42</sup> has a non-negligible influence on the output variables. This finding is of consequence since the effect of self-diffusivity parameters on the sensitivity of the Wilson–Frenkel interface kinetics model has not been explored in the literature before.

Building on the results from sensitivity analysis, the parametric estimation for both VTF and FPL diffusivity forms was conducted using the minimization of the sum of the least-squares approach. The lower and upper bounds for the parameters were specified as outlined in Table 2. The results for growth velocity as predicted by the optimized FPL and VTF forms are shown in Figure 9a,b. The values of the parameters taken as the initial guess and the optimized parameters for both forms are presented in Table 4. The comparison of the subplots in Figure 9 shows that both the diffusivity forms agree well with the experimental data of Wang et al.<sup>19</sup> and Shibkov et al.<sup>39</sup> for a supercooling degree lower than 8 K. In the kinetic-controlled regime, however, a significant discrepancy is observed between the two forms. The optimized solution parameters for the FPL diffusivity form deviates considerably with the experimental dendritic growth velocity for an undercooling degree  $>8$  K. It can also be observed that the difference between the optimized and initial guess in Figure 9a is negligible. This can be attributed to the relatively higher discrepancy in diffusivity of the FPL form with the experimental data at lower temperatures. This is also reported by Xu et al.<sup>43</sup> in a recent study, which observed that the FPL form has a higher deviation from the experimental diffusivity data for supercooled water at a temperature below 240 K. Furthermore, the limited range of applicability of the FPL parameters, as outlined in Table 2, also plays a role in limiting their accuracy in predicting the dendritic growth rate.

The VTF form, on the other hand, is able to predict the experimental data rather accurately for a supercooling degree of up to 30 K. Table 4 shows the final values of the optimized parameters and the objective function. The sum of least-squares for the VTF form was minimized up to 85%, as shown in Table 4. This demonstrates that the VTF form of diffusivity is more accurate in estimating the dendritic growth velocity and thus should be preferred while using the Wilson–Frenkel model to include interface kinetics effects.

While the Wilson–Frenkel model is physically rigorous in incorporating the kinetic effects in the crystal growth model of Lennard-Jones liquid,<sup>40</sup> a rather common and simplistic approach is using a linear kinetics model, as derived in the Methodology section (eq 13). Using the parametric estimation code, we were able to come up with the optimized value of the linear kinetic coefficient,  $\mu$ , for the dendritic growth of water. Figure 10 mirrors the results for the initial and optimized values of  $\mu$ . The initial value of  $\mu$  was taken from Kallungal et al.,<sup>36</sup> which demonstrated the kinetic constant for the ice growth along the  $a$ -axis to be 0.17 m/(s·K). The results of the initial guess and optimized model are also compared with the empirical correlation put forward by Cahn et al.<sup>31</sup> Results show that the optimized linear kinetics coefficient is able to predict the experimental data accurately in both diffusion-controlled and kinetic-controlled regimes. The results also depict the importance of adding curvature effects, as they improve the prediction further in the kinetic-controlled regime. The improvement in prediction is further quantified by the 87% reduction in the objective function, which was reduced from 0.91 to 0.12.

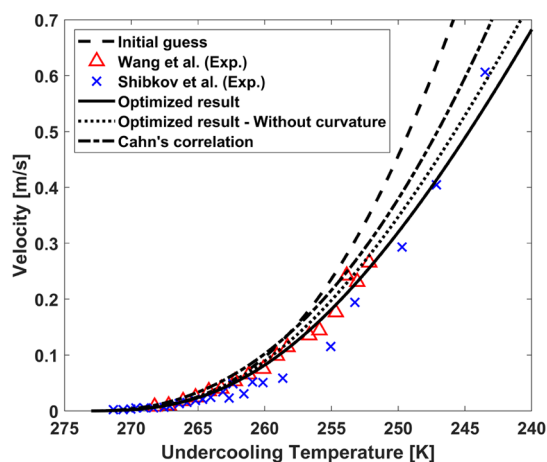


**Figure 10.** Dendritic growth velocity using the linear kinetics model. The optimized value of the linear kinetic coefficient,  $\mu$ , was calculated to be 0.067 m/(s·K). Experimental data shown here are within the error margin of 6%. The sum of least-squares between the experiments and simulation was 0.91 for the initial guess and 0.12 for the optimized  $\mu$ .

### Effect of Wilson–Frenkel Model Variants and Curvature.

The Wilson–Frenkel interface kinetics model for the growth rate of ice crystals in supercooled water, while more rigorous in its incorporation of kinetic effects, presents itself in several forms. Three of the most commonly used variants in the literature are derived in this work and presented in eqs 16–18. Using these variants in conjunction with eq 23, the resulting solution of dendritic growth velocity,  $v$ , is plotted against different undercooling temperatures,  $T_n$ , in Figure 11. It is important to note here that the variants studied in this section use the VTF diffusivity form with the optimized parameters, as presented in Table 4. Figure 11a exemplifies that while the variants do not differ appreciably in predicting the growth velocity,  $v$ , in the diffusion-controlled regime, the deviation is non-negligible for the undercooling temperature in the kinetic-controlled regime. This can be attributed to two main reasons. First, variant 3 uses the ideal gas assumption for the water vapor to model the saturation pressure. While this assumption holds well for higher undercooling temperatures, the water vapor deviates from the ideal gas behavior at lower temperatures. Second, the difference arises between variant 1 and 2 because of their varied treatment of the thermodynamic potential term in eq 15. The linearization of the exponential term causes the deviation especially at the lower values of undercooling temperatures. The effect of curvature on the growth velocity prediction is illuminated through the zoomed-in plot shown in Figure 11b. The plot elucidates that the curvature effects grow in significance as the undercooling temperature reduces. The reason for this lies in analyzing the evolution of the radius of the curvature with the growth velocity, as quantified by eq 21. A reduction in the undercooling temperature results in a smaller curvature radius,  $R$ , of the interface. This decrease in the radius of the curvature, in turn, causes the curvature undercooling term,  $\Delta T_c$ , to appreciate in the kinetic-controlled regime. This suggests that the curvature effects should be included especially if the undercooling temperature lies in the kinetic-controlled regime.

## CONCLUSIONS

The study presents a heterogeneous nucleation model for droplet freezing coupled with a novel approach to model

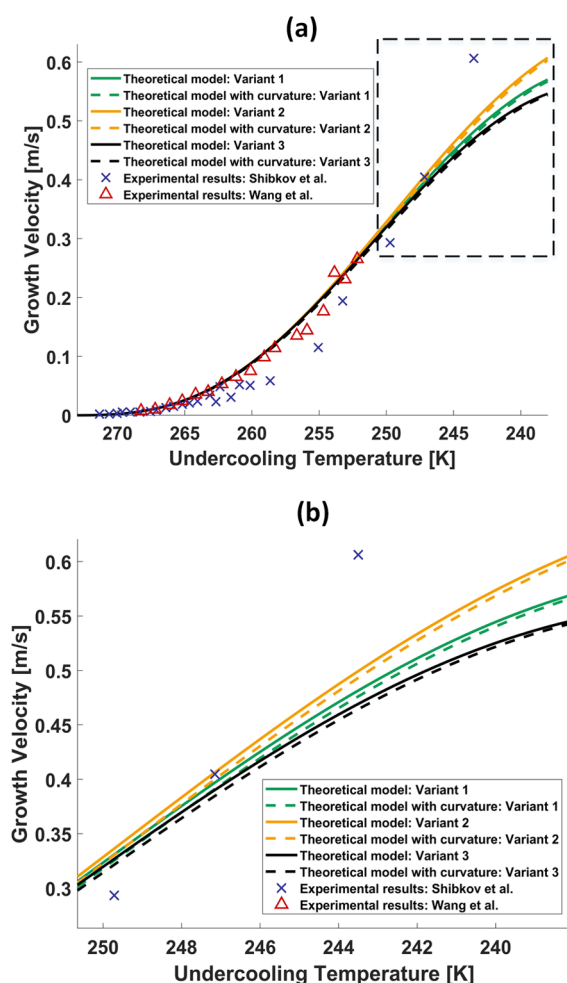


**Figure 11.** (a) Dendritic growth velocity,  $v$ , for three Wilson–Frenkel variants. Solid lines depict the solution without the curvature effects, whereas the dashed lines additionally include the curvature effects. The colors, yellow, green, and black, represent variants 1, 2, and 3, respectively. (b) Zoomed-in inset plot of the three variants highlighting the curvature effects in the kinetic-controlled regime.

dendritic growth that incorporates the effects of thermal diffusion, interface kinetics, and curvature undercooling on the dendritic growth rate. The study also develops a statistical framework to examine the sensitivity of the diffusion and kinetic model parameters on the output parameters of interest followed by their optimization. The findings of this study can be summarized as follows:

1. A heterogeneous nucleation model is developed to predict the nucleation delay for different surface hydrophobicities and different radii. The nucleation time is predicted to increase approximately twofold between the hydrophobic and superhydrophobic surfaces for the same radius. The nucleation time also increased linearly with the increase in the droplet volume.
2. The Wilson–Frenkel model is able to accurately predict the effect of interface kinetics on crystal growth. The accuracy, however, is not only a function of using an optimized value of the interface kinetics parameter,  $\beta$ , but also the form of diffusivity expression and the corresponding values of its parameters. This study finds the Vogel–Tamman–Fulcher (VTF) form of diffusivity, given in eq 19, to predict the crystal growth velocity

accurately. The Wilson–Frenkel model using the VTF diffusivity form compares well with the experimental data of Shibkov et al.<sup>39</sup> and Wang et al.,<sup>19</sup> both in diffusion-controlled and kinetic-controlled regimes.

3. The optimized values of both the Wilson–Frenkel model parameters and the linear interface kinetics coefficient are determined in this study. These estimated parameters can be used with confidence to predict dendritic growth velocities in supercooled water. Both dendritic growth models have been validated with two different experimental datasets and are valid for predicting the dendritic growth velocity and interface temperature for the supercooling degree of up to 30 K. This range of validity of the growth model has implications in accurately capturing the recalescence stage dynamics during the droplet freezing process, which finds its applications in a wide array of engineering and biological problems.
4. At higher undercoolings (>10 K), the radius of the curvature at the interface is reduced. This causes the curvature effects to be non-negligible at lower nucleation temperatures and thus they should be incorporated in the dendritic growth model.

## APPENDIX

The model for dendritic crystal growth presented in this paper is further applied to the undercooled melt of nickel using variant 1 of the Wilson–Frenkel model given by eq 16. Figure 12 shows

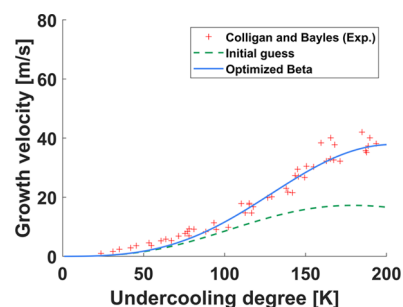


**Figure 12.** Dendritic growth velocity using variant 1 of the Wilson–Frenkel model. The initial guess for interface kinetic factor was assumed to be  $\beta = 1 \times 10^{-15}$  m. The optimized interface kinetic factor from the algorithm presented in this study is calculated to be  $\beta = 4.555 \times 10^{-16}$  m. Experimental results from Colligan and Bayles.<sup>65</sup>

the initial and optimized version of the model. The data for thermophysical and kinetic properties of Nickel are taken from Coriell and Turnbull,<sup>63</sup> whereas the expression for self-diffusivity of nickel is extracted from the experimental study by Maier et al.<sup>64</sup> Figure 13 compares the results of the present model and the LM-K model with the experimental data. The agreement clearly demonstrates that the current model is successfully able to predict crystal growth in other materials too.

## AUTHOR INFORMATION

### Corresponding Author

Agus P. Sasmito – Mining and Materials Engineering  
Department, McGill University, Montreal, Québec H3A 0C5,  
Canada; [orcid.org/0000-0003-3444-8922](https://orcid.org/0000-0003-3444-8922);  
Email: [agus.sasmito@mcgill.ca](mailto:agus.sasmito@mcgill.ca)

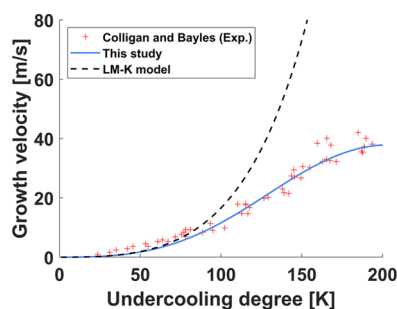


**Figure 13.** Comparison of results from the Wilson–Frenkel model with LM-K. Experimental results from Colligan and Bayles.<sup>65</sup>

## Authors

Saad Akhtar – Mining and Materials Engineering Department,  
McGill University, Montreal, Québec H3A 0C5, Canada

Minghan Xu – Mining and Materials Engineering Department,  
McGill University, Montreal, Québec H3A 0C5, Canada

Complete contact information is available at:  
<https://pubs.acs.org/10.1021/acs.cgd.0c01652>

## Notes

The authors declare no competing financial interest.

## ACKNOWLEDGMENTS

The first author would like to extend his gratitude to McGill Engineering Doctoral Award (MEDA) and Fonds de Recherche du Québec—Nature et Technologies (FRQNT)—Bourses de doctorat (B2X) for supporting this research. The computations for this study were conducted at the HPC facility under Calcul-Québec and Compute-Canada with contribution from CFI-JELF.

## ADDITIONAL NOTE

<sup>a</sup>Actual value of  $\beta$  is reported to be  $8 \times 10^{-10}$  by Xu et al.<sup>43</sup> However, their definition of  $\beta$  includes factor 6, as shown in eq 15. Hence it is divided by 6 here for consistency with our model.

## REFERENCES

- (1) Gao, P.; Cheng, B.; Zhou, X.; Zhang, D.; Zhou, G. Study on droplet freezing characteristic by ultrasonic. *Heat Mass Transfer* **2017**, *53*, 1725–1734.
- (2) Knopf, D. A.; Alpert, P. A.; Zipori, A.; Reicher, N.; Rudich, Y. Stochastic nucleation processes and substrate abundance explain time-dependent freezing in supercooled droplets. *npj Clim. Atmos. Sci.* **2020**, *3*, No. 2.
- (3) Dehghani-Sanij, A.; MacLachlan, S.; Naterer, G.; Muzychka, Y.; Haynes, R.; Enjilela, V. Multistage cooling and freezing of a saline spherical water droplet. *Int. J. Therm. Sci.* **2020**, *147*, No. 106095.
- (4) Vorontsov, D. A.; Sazaki, G.; Titaeva, E. K.; Kim, E. L.; Bayer-Giraldi, M.; Furukawa, Y. Growth of Ice Crystals in the Presence of Type III Antifreeze Protein. *Cryst. Growth Des.* **2018**, *18*, 2563–2571.
- (5) Knight, C. A.; Wierzbicki, A. Adsorption of Biomolecules to Ice and Their Effects upon Ice Growth. 2. A Discussion of the Basic Mechanism of “Antifreeze” Phenomena. *Cryst. Growth Des.* **2001**, *1*, 439–446.
- (6) Kishimoto, T.; Sekozawa, Y.; Yamazaki, H.; Murakawa, H.; Kuchitsu, K.; Ishikawa, M. Seasonal changes in ice nucleation activity in blueberry stems and effects of cold treatments in vitro. *Environ. Exp. Bot.* **2014**, *106*, 13–23.
- (7) Hindmarsh, J.; Russell, A.; Chen, X. Fundamentals of the spray freezing of foods-microstructure of frozen droplets. *J. Food Eng.* **2007**, *78*, 136–150.

(8) Sebastião, I. B.; Bhatnagar, B.; Tchessalov, S.; Ohtake, S.; Plitzko, M.; Luy, B.; Alexeenko, A. Bulk dynamic spray freeze-drying part 1: modeling of droplet cooling and phase change. *J. Pharm. Sci.* **2019**, *108*, 2063–2074.

(9) Lee, G. W.; Jeon, S.; Kang, D. H. Crystal-liquid interfacial free energy of supercooled liquid Fe using a containerless technique. *Cryst. Growth Des.* **2013**, *13*, 1786–1792.

(10) Liu, S.; Li, H.; Song, M.; Dai, B.; Sun, Z. Impacts on the solidification of water on plate surface for cold energy storage using ice slurry. *Appl. Energy* **2018**, *227*, 284–293.

(11) Meng, Z.; Zhang, P. Dynamic propagation of ice-water phase front in a supercooled water droplet. *Int. J. Heat Mass Transfer* **2020**, *152*, No. 119468.

(12) Zhao, Y.; Guo, Q.; Lin, T.; Cheng, P. A review of recent literature on icing phenomena: Transport mechanisms, their modulations and controls. *Int. J. Heat Mass Transfer* **2020**, *159*, No. 120074.

(13) Hindmarsh, J. P.; Russell, A. B.; Chen, X. D. Experimental and numerical analysis of the temperature transition of a suspended freezing water droplet. *Int. J. Heat Mass Transfer* **2003**, *46*, 1199–1213.

(14) Akhtar, S.; Xu, M.; Sasmito, A. P. Development and validation of an asymptotic solution for a two-phase Stefan problem in a droplet subjected to convective boundary condition. *Int. J. Therm. Sci.* **2021**, *164*, No. 106923.

(15) Lindenmeyer, C. S.; Orrok, G. T.; Jackson, K. A.; Chalmers, B. Rate of growth of ice crystals in supercooled water. *J. Chem. Phys.* **1957**, *27*, 822.

(16) Frenkel, J. Note on a relation between the speed of crystallization and viscosity. *Physik. Zeit. Sowjetunion* **1932**, *1*, 498–510.

(17) Wilson, H. W. XX. On the velocity of solidification and viscosity of super-cooled liquids. *Philos. Mag.* **1900**, *50*, 238–250.

(18) Buttersack, T.; Bauerecker, S. Critical radius of supercooled water droplets: On the transition toward dendritic freezing. *J. Phys. Chem. B* **2016**, *120*, 504–512.

(19) Wang, T.; Lü, Y.; Ai, L.; Zhou, Y.; Chen, M. Dendritic Growth Model Involving Interface Kinetics for Supercooled Water. *Langmuir* **2019**, *35*, 5162–5167.

(20) Bauerecker, S.; Buttersack, T. Electric effect during the fast dendritic freezing of supercooled water droplets. *J. Phys. Chem. B* **2014**, *118*, 13629–13635.

(21) Wang, Y.; Cheng, Y. New perspectives on the droplet freezing nucleation and early crystal growth mechanisms. *Int. J. Heat Mass Transfer* **2019**, *140*, 1023–1028.

(22) Boinovich, L.; Emelyanenko, A. M.; Korolev, V. V.; Pashinin, A. S. Effect of wettability on sessile drop freezing: When superhydrophobicity stimulates an extreme freezing delay. *Langmuir* **2014**, *30*, 1659–1668.

(23) Schutzius, T. M.; Jung, S.; Maitra, T.; Eberle, P.; Antonini, C.; Stamatoopoulos, C.; Poulikakos, D. Physics of icing and rational design of surfaces with extraordinary icephobicity. *Langmuir* **2015**, *31*, 4807–4821.

(24) Nakaya, U. *Snow Crystals*; Harvard University Press, 2013.

(25) Libbrecht, K. G. Physical Dynamics of Ice Crystal Growth. *Annu. Rev. Mater. Res.* **2017**, *47*, 271–295.

(26) Jung, S.; Tiwari, M. K.; Doan, N. V.; Poulikakos, D. Mechanism of supercooled droplet freezing on surfaces. *Nat. Commun.* **2012**, *3*, No. 615.

(27) Gai, S.; Peng, Z.; Moghtaderi, B.; Yu, J.; Doroodchi, E. LBM modelling of supercooled water freezing with inclusion of the recalescence stage. *Int. J. Heat Mass Transfer* **2020**, *146*, No. 118839.

(28) Jackson, K. A. The interface kinetics of crystal growth processes. *Interface Sci.* **2002**, *10*, 159–169.

(29) Jackson, K. A. *Kinetic Processes: Crystal Growth, Diffusion, and Phase Transformations in Materials*; John Wiley & Sons, 2006; pp 351–359.

(30) Kapembwa, M.; Rodríguez-Pascual, M.; Lewis, A. E. Heat and mass transfer effects on ice growth mechanisms in pure water and aqueous solutions. *Cryst. Growth Des.* **2014**, *14*, 389–395.

(31) Cahn, J. W.; Hillig, W. B.; Sears, G. W. The molecular mechanism of solidification. *Acta Metall.* **1964**, *12*, 1421–1439.

- (32) Papapetrou, A. Studies on the dendritic growth of crystals. *Z. Kristallogr.* **1935**, *92*, 89–130.
- (33) Ivantsov, G. Temperature field around a spherical, cylindrical, and needle-shaped crystal, growing in a pre-cooled melt. *NASA TM-77889* **1985**, *58*, 567–569.
- (34) Langer, J. S.; Müller-Krumbhaar, J. Stability effects in dendritic crystal growth. *J. Cryst. Growth* **1977**, *42*, 11–14.
- (35) Langer, J.; Sekerka, R.; Fujioka, T. Evidence for a universal law of dendritic growth rates. *J. Cryst. Growth* **1978**, *44*, 414–418.
- (36) Kallungal, J. P.; Barduhn, A. J. Growth rate of an ice crystal in subcooled pure water. *AIChE J.* **1977**, *23*, 294–303.
- (37) Trivedi, R.; Kurz, W. Morphological stability of a planar interface under rapid solidification conditions. *Acta Metall.* **1986**, *34*, 1663–1670.
- (38) Shibkov, A. A.; Golovin, Y. I.; Zheltov, M. A.; Korolev, A. A.; Leonov, A. A. Morphology diagram of nonequilibrium patterns of ice crystals growing in supercooled water. *Phys. A* **2003**, *319*, 65–79.
- (39) Shibkov, A. A.; Zheltov, M. A.; Korolev, A. A.; Kazakov, A. A.; Leonov, A. A. Crossover from diffusion-limited to kinetics-limited growth of ice crystals. *J. Cryst. Growth* **2005**, *285*, 215–227.
- (40) Broughton, J. Q.; Gilmer, G. H.; Jackson, K. A. Crystallization rates of a Lennard-Jones liquid. *Phys. Rev. Lett.* **1982**, *49*, 1496–1500.
- (41) Markov, I. V. Crystal Growth for Beginners. *World Sci.* **2003**, 77–179.
- (42) Price, W. S.; Ide, H.; Arata, Y. Self-diffusion of supercooled water to 238 K using PGSE NMR diffusion measurements. *J. Phys. Chem. A* **1999**, *103*, 448–450.
- (43) Xu, Y.; Petrik, N. G.; Smith, R. S.; Kay, B. D.; Kimmel, G. A. Growth rate of crystalline ice and the diffusivity of supercooled water from 126 to 262 K. *Proc. Natl. Acad. Sci. U.S.A.* **2016**, *113*, 14921–14925.
- (44) Prielmeier, F. X.; Lang, E. W.; Speedy, R. J.; Ldemann, H. D. Diffusion in supercooled water to 300 MPa. *Phys. Rev. Lett.* **1987**, *59*, 1128–1131.
- (45) Vehkamäki, H.; Määttänen, A.; Lauri, A.; Napari, I.; Kulmala, M. Technical Note: The heterogeneous Zeldovich factor. *Atmos. Chem. Phys.* **2007**, *7*, 309–313.
- (46) Alizadeh, A.; Yamada, M.; Li, R.; Shang, W.; Otta, S.; Zhong, S.; Ge, L.; Dhinojwala, A.; Conway, K. R.; Bahadur, V.; Vinciguerra, A. J.; Stephens, B.; Blohm, M. L. Dynamics of Ice Nucleation on Water Repellent Surfaces. *Langmuir* **2012**, *28*, 3180–3186.
- (47) McFadden, G. B.; Wheeler, A. A.; Braun, R. J.; Coriell, S. R.; Sekerka, R. F. Phase-field models for anisotropic interfaces. *Phys. Rev. E* **1993**, *48*, 2016–2024.
- (48) Mills, A. *Basic Heat and Mass Transfer*; Prentice Hall, 1999.
- (49) Hobbs, P. V. *Ice Physics*; Oxford University Press, 2010.
- (50) Tanaka, K. K.; Kimura, Y. Theoretical analysis of crystallization by homogeneous nucleation of water droplets. *Phys. Chem. Chem. Phys.* **2019**, *21*, 2410–2418.
- (51) Coriell, S.; Hardy, S.; Sekerka, R. A non-linear analysis of experiments on the morphological stability of ice cylinders freezing from aqueous solutions. *J. Cryst. Growth* **1971**, *11*, 53–67.
- (52) Murphy, D. M.; Koop, T. Review of the vapour pressures of ice and supercooled water for atmospheric applications. *Q. J. R. Meteorol. Soc.* **2005**, *131*, 1539–1565.
- (53) Knight, C. Structural Approach to Ice Growth (and Nucleation) in Liquid Water. *Cryst. Growth Des.* **2020**, *20*, 580–589.
- (54) Boettinger, W.; Coriell, S. *Science and Technology of the Undercooled Melt*; Springer, 1986; pp 81–109.
- (55) Lipton, J.; Kurz, W.; Trivedi, R. Rapid Dendrite Growth in Undercooled Alloys. *Acta Metall.* **1987**, *35*, 957–964.
- (56) Yong-Jun, L.; Xie, W. J.; Wei, B. B. Rapid growth of ice dendrite in acoustically levitated and highly undercooled water. *Chin. Phys. Lett.* **2002**, *19*, 1543–1546.
- (57) Rozmanov, D.; Kusalik, P. G. Temperature dependence of crystal growth of hexagonal ice (I h). *Phys. Chem. Chem. Phys.* **2011**, *13*, 15501–15511.
- (58) Lamanna, R.; Delmelle, M.; Cannistraro, S. Role of hydrogen-bond cooperativity and free-volume fluctuations in the non-Arrhenius behavior of water self-diffusion: A continuity-of-states model. *Phys. Rev. E* **1994**, *49*, 2841–2850.
- (59) Gillen, K. T.; Douglass, D. C.; Hoch, M. J. Self-diffusion in liquid water to  $-31^{\circ}\text{C}$ . *J. Chem. Phys.* **1972**, *57*, 5117–5119.
- (60) Kendall, M.; Stuart, A. *The Advanced Theory of Statistics: Design and Analysis, and Time-Series*; Griffin, 1976.
- (61) Zar, J. H. Significance testing of the Spearman rank correlation coefficient. *J. Am. Stat. Assoc.* **1972**, *67*, 578–580.
- (62) Cao, L.; Jones, A. K.; Sikka, V. K.; Wu, J.; Gao, D. Anti-Icing superhydrophobic coatings. *Langmuir* **2009**, *25*, 12444–12448.
- (63) Coriell, S.; Turnbull, D. Relative roles of heat transport and interface rearrangement rates in the rapid growth of crystals in undercooled melts. *Acta Metall.* **1982**, *30*, 2135–2139.
- (64) Maier, K.; Mehrer, H.; Lessmann, E.; Schüle, W. Self-diffusion in nickel at low temperatures. *Phys. Status Solidi B* **1976**, *78*, 689–698.
- (65) Colligan, G.; Bayles, B. Dendrite growth velocity in undercooled nickel melts. *Acta Metall.* **1962**, *10*, 895–897.